3 1176 00092 9043

C.2

NACA RM A58H12

NACA

RESEARCH MEMORANDUM

LARGE-SCALE WIND-TUNNEL TESTS OF A JET-TRANSPORT-TYPE MODEL WITH LEADING- AND TRAILING-EDGE HIGH-LIFT DEVICES

By David H. Hickey and Kiyoshi Aoyagi

Ames Aeronautical Laboratory
Moffett Field, Calif.

LIBRARY COPY

SEP 29 1958

LANGLEY AERONAUTICAL LABORATORY
LIBRARY, NACA
LANGLEY FIELD, VIRGINIA

NATIONAL ADVISORY COMMITTEE
FOR AERONAUTICS

WASHINGTON

September 26, 1958

NATIONAL ADVISORY COMMITTEE FOR AERONAUTICS

RESEARCH MEMORANDUM

LARGE-SCALE WIND-TUNNEL TESTS OF A JET-TRANSPORT-TYPE MODEL WITH LEADING- AND TRAILING-EDGE HIGH-LIFT DEVICES

By David H. Hickey and Kiyoshi Aoyagi

SUMMARY

An investigation was conducted to determine the longitudinal characteristics of an airplane model with a 35° swept wing of aspect ratio 7 and four pylon-mounted nacelles. Several leading-edge configurations were studied in conjunction with double-slotted trailing-edge flaps.

Three-component longitudinal data are presented. In general, the test Reynolds number was about 4.8×10^6, but for selected configurations, data for Reynolds number ranges from 2.8 to 8×10^6 are included.

INTRODUCTION

A study of the low-speed longitudinal characteristics of a jet-transport model with a swept wing and four pylon-mounted nacelles is being conducted in the Ames 40- by 80-foot wind tunnel. Results were obtained with double-slotted trailing-edge flaps, a slatted leading edge, and a leading edge with increased camber and airfoil nose radius.

Data from the initial investigation are presented herein. The majority of the data were obtained at a Reynolds number of 4.8 million. Some configurations were tested with Reynolds numbers ranging from 2.8 to 8 million.

The results are presented without discussion in order to expedite publication.

NOTATION

b	wing span, ft
c	wing chord parallel to the line of symmetry, ft
$\bar{c}$	mean aerodynamic chord, $\frac{\int_0^{b/2} c^2 dy}{\int_0^{b/2} c\, dy}$, ft
C_L	lift coefficient, $\frac{\text{lift}}{q_\infty S}$
C_D	drag coefficient, $\frac{\text{drag}}{q_\infty S}$
C_m	pitching-moment coefficient about $0.25\bar{c}$, $\frac{\text{moment}}{q_\infty S\bar{c}}$
i_t	horizontal-tail incidence angle, deg
LE	leading edge
MLE	modified leading edge
q_∞	free-stream dynamic pressure, lb/sq ft
R	Reynolds number, $\frac{V_\infty \bar{c}}{\nu}$
V_∞	free-stream air velocity, ft/sec
x	distance along the chord line from the airfoil leading edge to some point on the airfoil, ft
y	spanwise distance perpendicular to the plane of symmetry, ft
z	perpendicular distance from the chord line to the airfoil surface, ft
δ_f	deflection of the main trailing-edge flap measured perpendicular to the hinge line, deg
δ_s	slat deflection measured perpendicular to the leading edge, deg
ν	free-stream kinematic viscosity, ft^2/sec
η	fraction of wing semispan, $\frac{2y}{b}$

Subscripts

f main trailing-edge flap

l lower surface

u upper surface, or uncorrected

v trailing-edge flap vane

MODEL

Figure 1 is a photograph of the model as installed in the 40- by 80-foot wind tunnel and figure 2 is a sketch of the model giving pertinent dimensions.

Wing Geometry

The wing had an aspect ratio of 7, taper ratio of 0.3, and sweepback of 35°, 6° of dihedral, and a 2° incidence angle. The basic airfoil section at the root was 65-A414, tapering to a 65A410 at the tip (see table I). A portion of the wing ahead of the 20-percent chord line and behind the 60-percent chord line was removable so that different leading edges and trailing edges could be tested.

Wing Leading Edges

The basic wing leading edge was constructed so that the forward portion of the wing could be deflected as a slat. Pertinent dimensions of the slat arrangement are shown in figure 3(a), and slat coordinates are given in table II. The slat was deflected 15° when in the extended position. Different spanwise slat extents were tested. The spanwise extent of the extended slat is specified on the figures as follows: δ_s (0.09 - 1.0). This means that the slat was extended between $\eta = 0.09$ and 1.0.

Another leading edge incorporating both increased camber upstream from the 20-percent line and increased leading-edge radius was tested (see table III for ordinates). The camber varied spanwise to give the wing chord lines 3° of geometric twist (see fig. 3(b)). The leading-edge radius was increased from normal at the root section to 0.02 chord at $\eta = 0.4$. From $\eta = 0.4$ outboard, the leading-edge radius was a constant 0.02 chord. This leading edge is referred to on the figures as MLE (modified leading edge).

A 0.15 chord Kruger flap, extending from $\eta = 0.55$ to 0.7 was tested. The flap was contoured to the lower surface airfoil shape and was deflected 50°.

Trailing-Edge Flap

The double-slotted trailing-edge flap used on the model was similar to that studied in reference 1. Pertinent dimensions of the flap are shown in figure 4, and flap ordinates are shown in table IV. A typical flap configuration is described on the figures as $\delta_f = 50^\circ$ (0.09 - 0.63). This means that the flap was deflected 50° between $\eta = 0.09$ and 0.63.

Fuselage

The fuselage cross section was defined by a 4- by 5-foot ellipse, except for the nose and the tail cone. The nose section was a 4- by 8-foot ellipse in the horizontal cross section and a 5- by 8-foot ellipse in the vertical cross section. The tail cone had a straight taper from a 4- by 5-foot ellipse to a similar but smaller ellipse at the tail.

Nacelles

Engine nacelles used in this test were designed to house J-30 engines for thrust-reverser tests. Unless otherwise specified, the nacelles and pylons were mounted on the model.

Tail

Geometry of the horizontal and vertical tails is described in figure 2. Incidence of the horizontal tail could be changed from +4° to -8°. The vertical tail was fixed. Unless otherwise specified, the tail was mounted on the model.

CORRECTIONS

The following corrections for the effects of wind-tunnel-wall interference were applied:

$$\alpha = \alpha_u + 0.59 \ C_L$$

$$C_D = C_{D_u} + 0.010 \ C_L^2$$

$$C_m = C_{m_u} + 0.0028 \ C_L \text{ (tail on)}$$

RESULTS

Three-component longitudinal data were measured at zero sideslip angle.

Figures 5 through 7 present data showing the effect of different leading-edge configurations on the longitudinal characteristics of the model. Results with and without full-span slats and with the modified leading edge are included in figure 5. The effect of several spanwise extents of leading-edge slat is shown in figure 6. Results presented in figure 7 are for the plain leading edge, an extended slat between the nacelles, and a 0.15η Kruger flap inboard of the outboard nacelle. The trailing-edge flap was deflected 50° for these data.

Figures 8 through 10 present data showing the effect of trailing-edge flap configuration variables on longitudinal characteristics. Variables considered are trailing-edge flap deflection with and without slats and with the modified leading edge (fig. 8), flap spanwise extent (fig. 9), and blocked flap slots (fig. 10).

Data in figure 11 show the effect on longitudinal characteristics of tail incidence and absence of the tail. Data in figure 12 show the effect of nacelles and pylons on the longitudinal characteristics of the model. Results are presented with and without pylons and nacelles for three leading-edge configurations and three trailing-edge flap deflections.

Data showing longitudinal characteristics for Reynolds numbers from 2.8 to 8.1 million are presented in figures 13 and 14. Results for two leading-edge configurations and two trailing-edge flap configurations, all with nacelles on, are included. Figure 15 shows similar results without nacelles and pylons for the modified leading edge and two trailing-edge flap deflections.

Ames Aeronautical Laboratory
National Advisory Committee for Aeronautics
Moffett Field, Calif., Aug. 12, 1958

REFERENCE

1. Naeseth, Rodger L.: Effect of a Fuselage on the Low-Speed Longitudinal Aerodynamic Characteristics of a 45° Sweptback Wing With Double-Slotted Flaps. NACA RM L56G02, 1956.

TABLE I.- COORDINATES OF BASIC WING PARALLEL TO THE MODEL PLANE OF SYMMETRY

x_u/c	z_u/c		x_l/c	z_l/c	
	$\eta = 0$	$\eta = 1.0$		$\eta = 0$	$\eta = 1.0$
0	0	0	0	0	0
.00347	.01178	.00842	.00653	-.00945	-.00675
.0058	.01442	.0103	.00920	-.01115	-.00797
.01059	.01853	.01323	.01441	-.01353	-.00967
.02283	.02606	.01862	.02717	-.01738	-.01242
.04757	.03765	.02689	.05243	-.02290	-.01636
.07247	.04678	.03342	.07753	-.02700	-.01928
.09746	.05451	.03893	.10254	-.03038	-.02170
.14757	.06698	.04784	.15243	-.03557	-.02541
.19781	.07656	.05468	.20219	-.03941	-.02815
.24811	.08392	.05994	.25189	-.04215	-.03011
.29846	.08934	.06382	.30154	-.04398	-.03142
.34884	.09299	.06642	.35116	-.04493	-.03209
.39923	.09495	.06782	.40077	-.04497	-.03212
.44962	.09495	.06782	.45038	-.04385	-.03132
.5000	.09290	.06636	.50000	-.04143	-.02959
.55035	.08869	.06335	.54965	-.0376	-.02685
.60064	.08266	.05904	.59936		
.65086	.07513	.05367	.64914		
.70101	.06634	.04738	.69899		
.75107	.05655	.04039	.74893		
.80103	.04591	.03279	.79897		
.85090	.03470	.02478	.84910		
.90066	.02309	.01649	.89934		
.95033	.01150	.00822	.94967		
1.000	0	0	1.00000	0	0

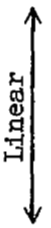

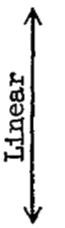

TABLE II.- COORDINATES OF INSIDE SLAT[1] AND WING PARALLEL TO THE MODEL PLANE OF SYMMETRY

[Outside coordinates are the same as those in table I]

x/c	η = 0		η = 1.0	
	Slat z/c	Wing z/c	Slat z/c	Wing z/c
0.02262	-0.01592	-0.01592	-0.01183	-0.01183
.02283	-.01213	-.01460	-.00908	-.01045
.04757	.01873	.01345	.01320	.00935
.07247	.03284	.02945	.02365	.02063
.09746	.04505	.04266	.03190	.02943
.14757	.06526	.06526	.04510	.04318

[1]Slat trailing edge at x/c = 0.1555

TABLE III.- MODIFIED LEADING-EDGE COORDINATES PARALLEL TO THE MODEL PLANE OF SYMMETRY

x/c	η = 0		η = 0.4		η = 1.0	
	z_u/c	z_l/c	z_u/c	z_l/c	z_u/c	z_l/c
0	0.01774	0.01774	0.00894	0.00894	-0.03493	-0.03493
.00347	.02665	.00908	.02372	.00011	-.01953	-.04400
.0058	.02863	.00718	.02601	-.00241	-.01678	-.04620
.01059	.03176	.00413	.02979	-.00607	-.01210	-.04951
.02283	.03754	-.00149	.03541	-.00985	-.00358	-.05143
.04757	.04637	-.00998	.04389	-.01627	.00990	-.04675
.07247	.05322	-.01675	.05053	-.02086	.02063	-.04263
.09746	.05916	-.02252	.05615	-.02521	.02915	-.03850
.14757	.06856	-.03152	.06532	-.03163	.04483	-.03163
.20000	.07657	-.03919	.07288	-.03713	.05473	-.02778

TABLE IV.- DOUBLE-SLOTTED TRAILING-EDGE-FLAP COORDINATES PARALLEL TO THE MODEL PLANE OF SYMMETRY

x/c_f	Main flap				Vane		
	η = 0.089		η = 0.626				
	z_u/c_f	z_l/c_f	z_u/c_f	z_l/c_f	x/c_v	z_u/c_v	z_l/c_v
0	-0.0273	-0.0273	-0.0106	-0.0106	0	0	0
.0125	.008	-.0533	.0252	-.0401	.0125	.0381	-.0268
.025	.028	-.0608	.0416	-.0477	.025	.0522	-.0339
.05	.0588	-.0651	.0659	-.0531	.05	.0739	-.0409
.075	.0815	-.0659	.0838	-.0547	.075	.0905	-.0446
.10	.0990	-.0659	.0984	-.0547	.10	.1050	-.0480
.15	.1248	-.0639	.1200	-.0522	.15	.1269	-.0409
.20	.1412	-.0593	.1339	-.0486	.20	.1440	-.0300
.30	.1528	-.0489	.1430	-.0401	.30	.1630	-.0140
.40	.1492	-.0395	.1391	-.0316	.40	.1660	.0010
.50	.1275	-.0320	.1200	-.0258	.50	.1600	.0180
.60	.1026	-.0255	.0969	-.0206	.60	.1440	.0300
.70	.0775	-.0187	.0741	-.0152	.70	.1170	.0320
.80	.0519	-.0129	.0498	-.0103	.80	.0830	.0200
.90	.0266	-.0069	.0255	-.0058	.90	.0450	.0180
.95	.0135	-.0040	.0134	-.0033	.95	.0260	.0107
1.00	.0009	-.0009	.0006	-.0006	1.00	0	0

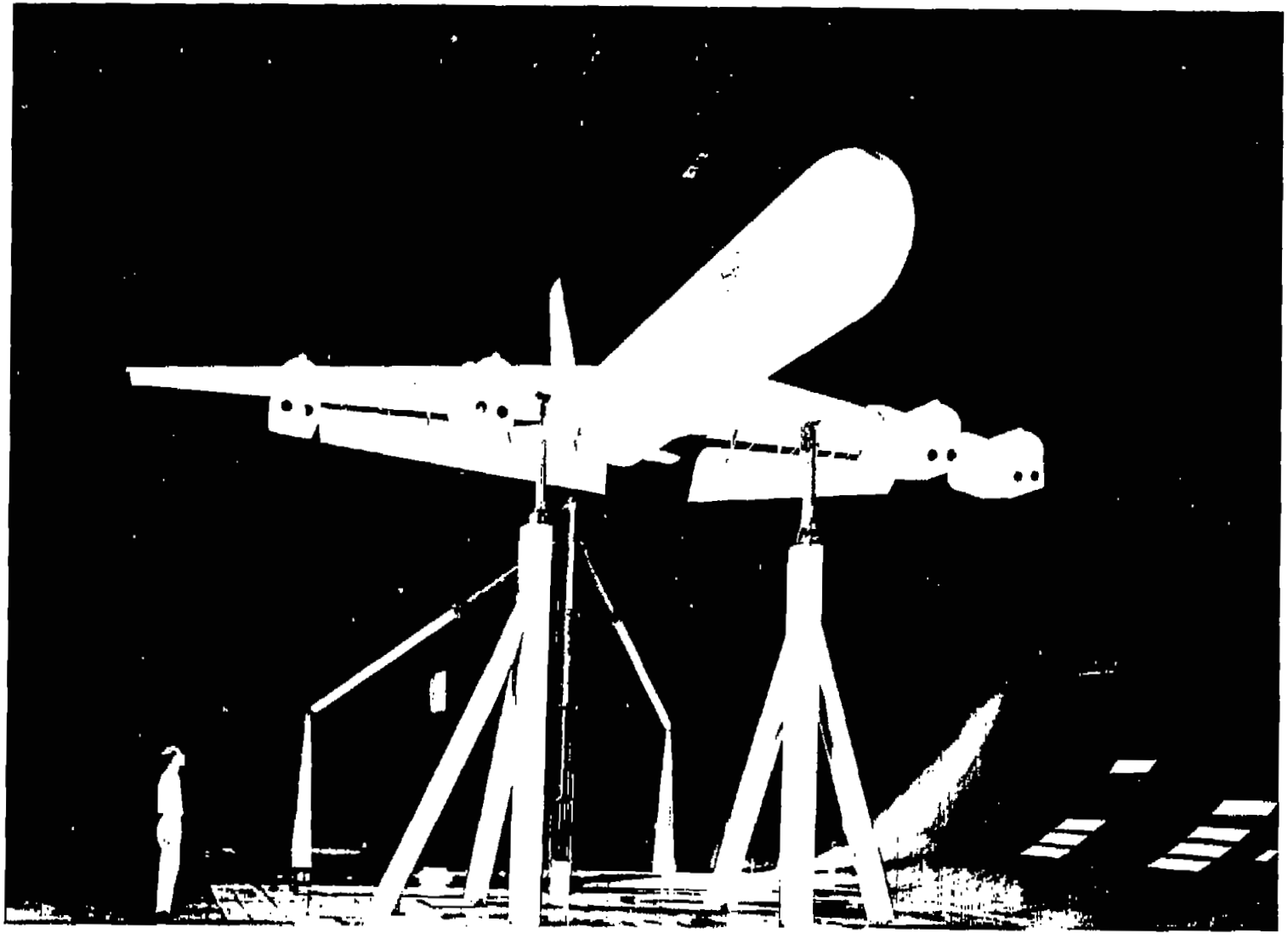

A-23878

Figure 1.- Large-scale model mounted in the Ames 40- by 80-foot wind tunnel.

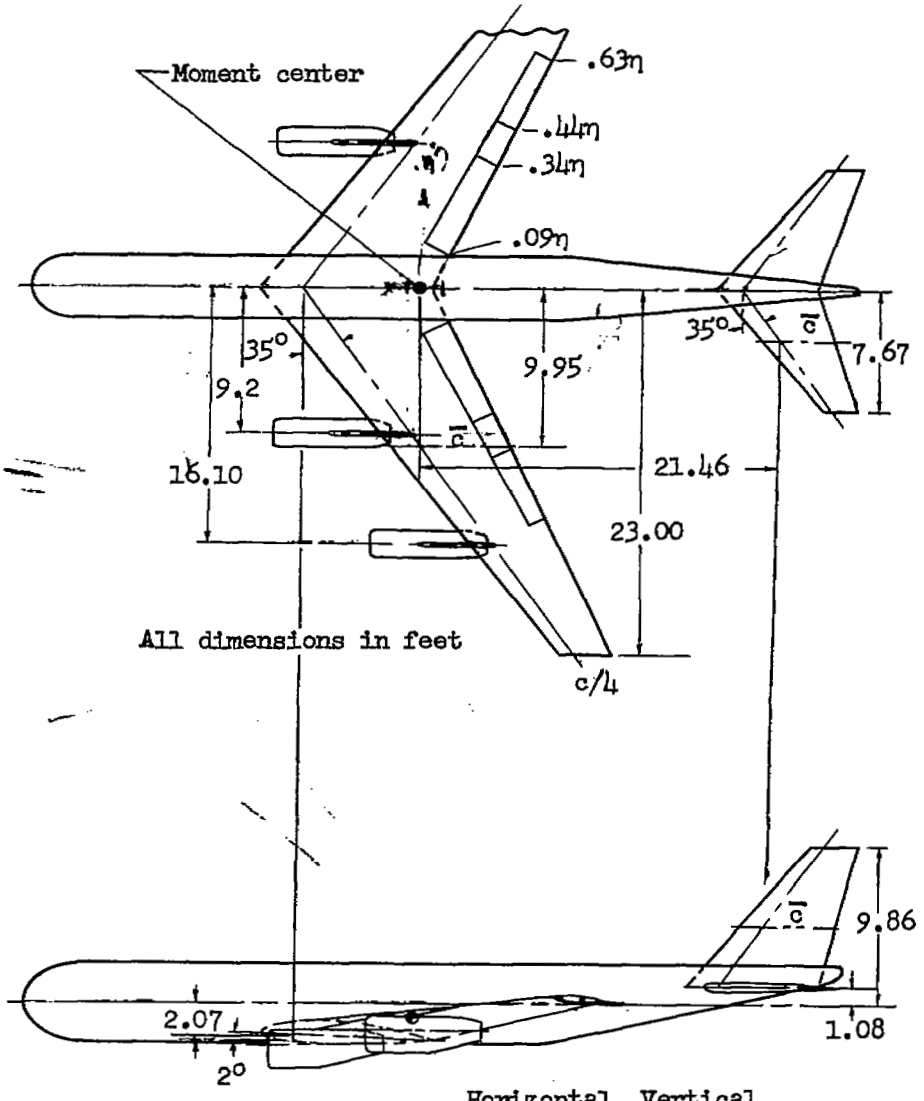

	Wing	Horizontal tail	Vertical tail
Aspect ratio	7.0	3.7	3.3
Taper ratio	0.3	0.375	0.359
Area, sq ft	302.0	62.8	46.7
Mean aerodynamic chord, ft	7.15	4.39	5.72
Dihedral, deg	6	0	- -

Figure 2.- Geometric details of the model.

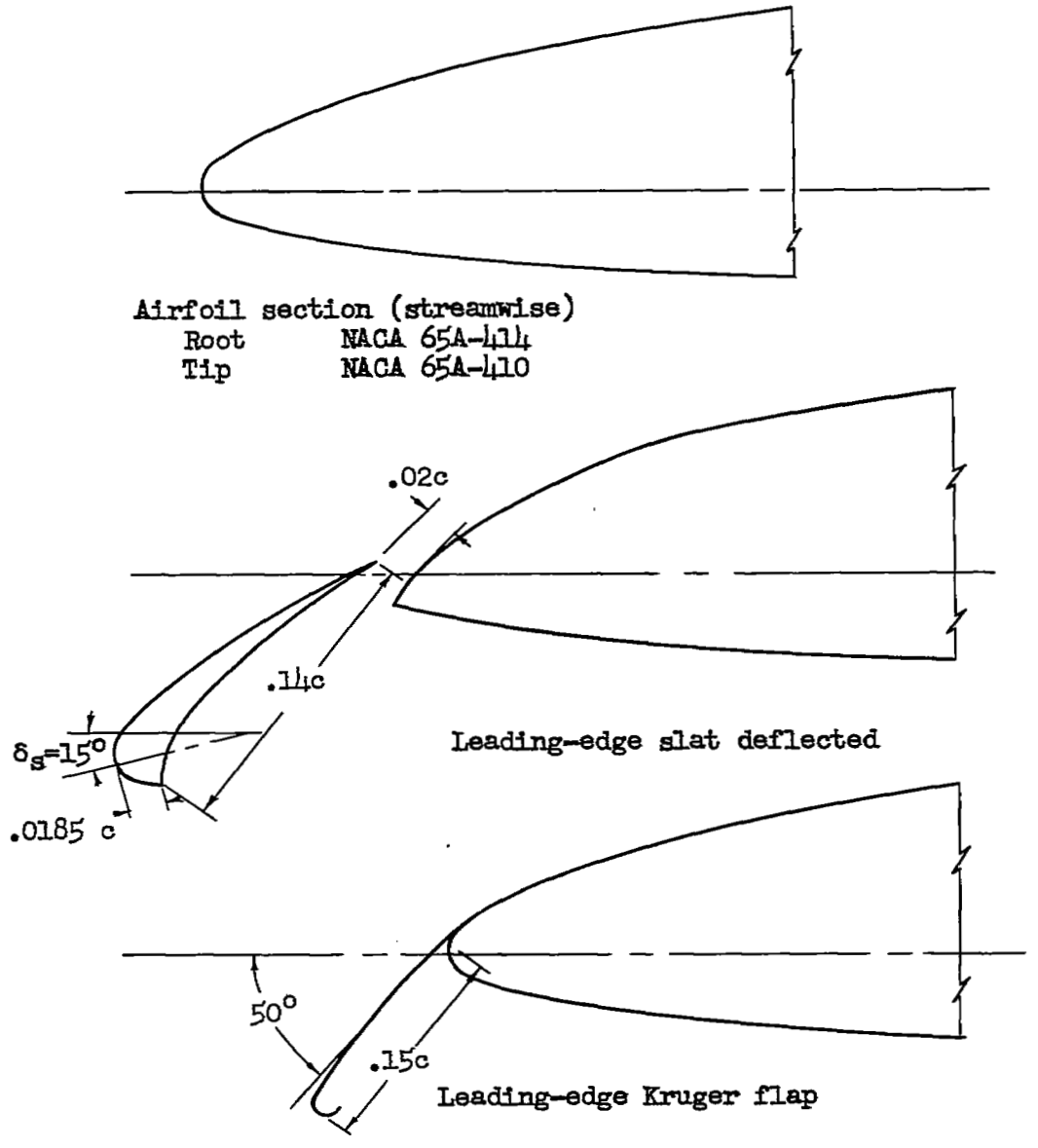

(a) Basic airfoil leading edge.

Figure 3.- Details of the leading edges tested.

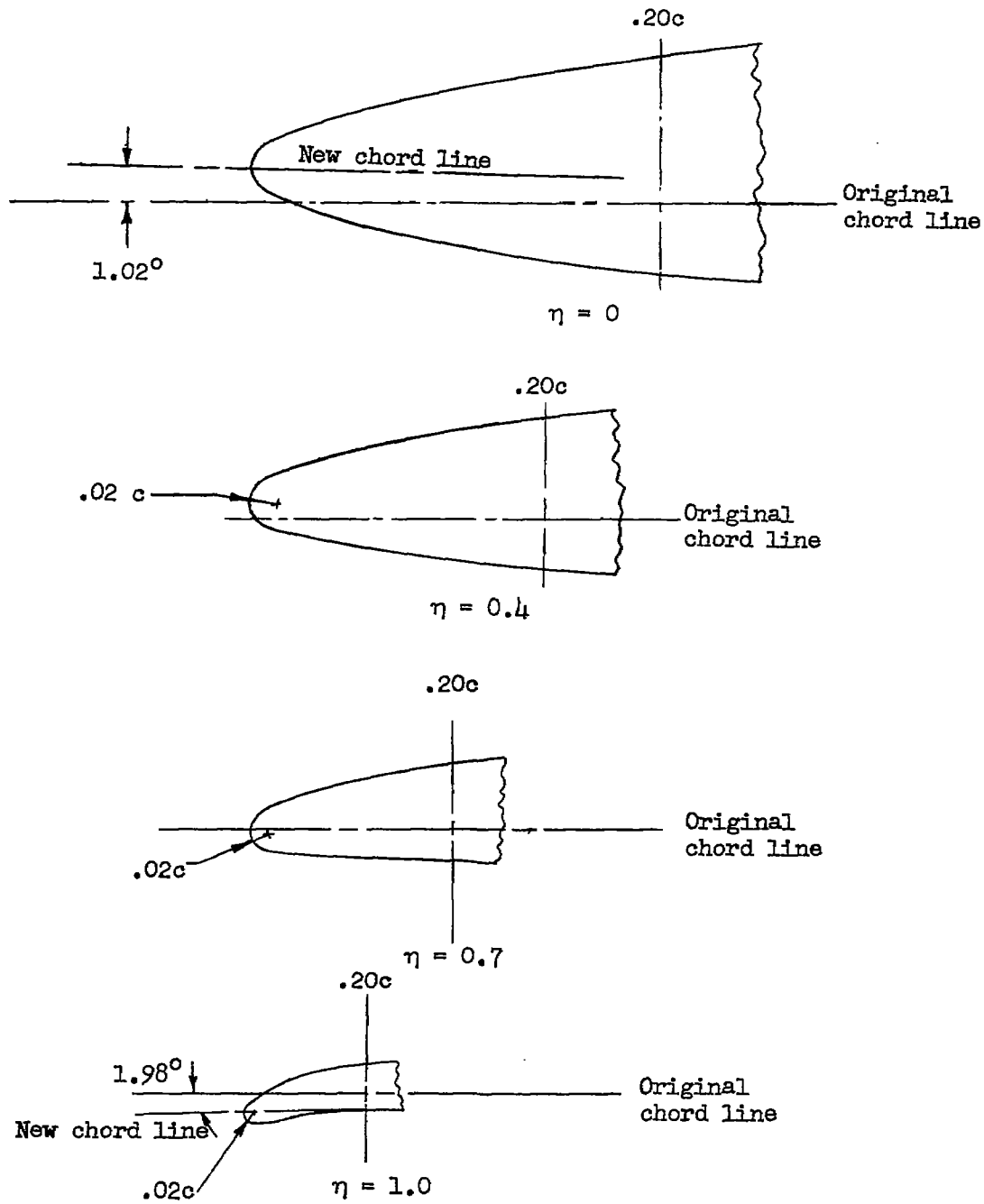

(b) Modified leading edge.

Figure 3.- Concluded.

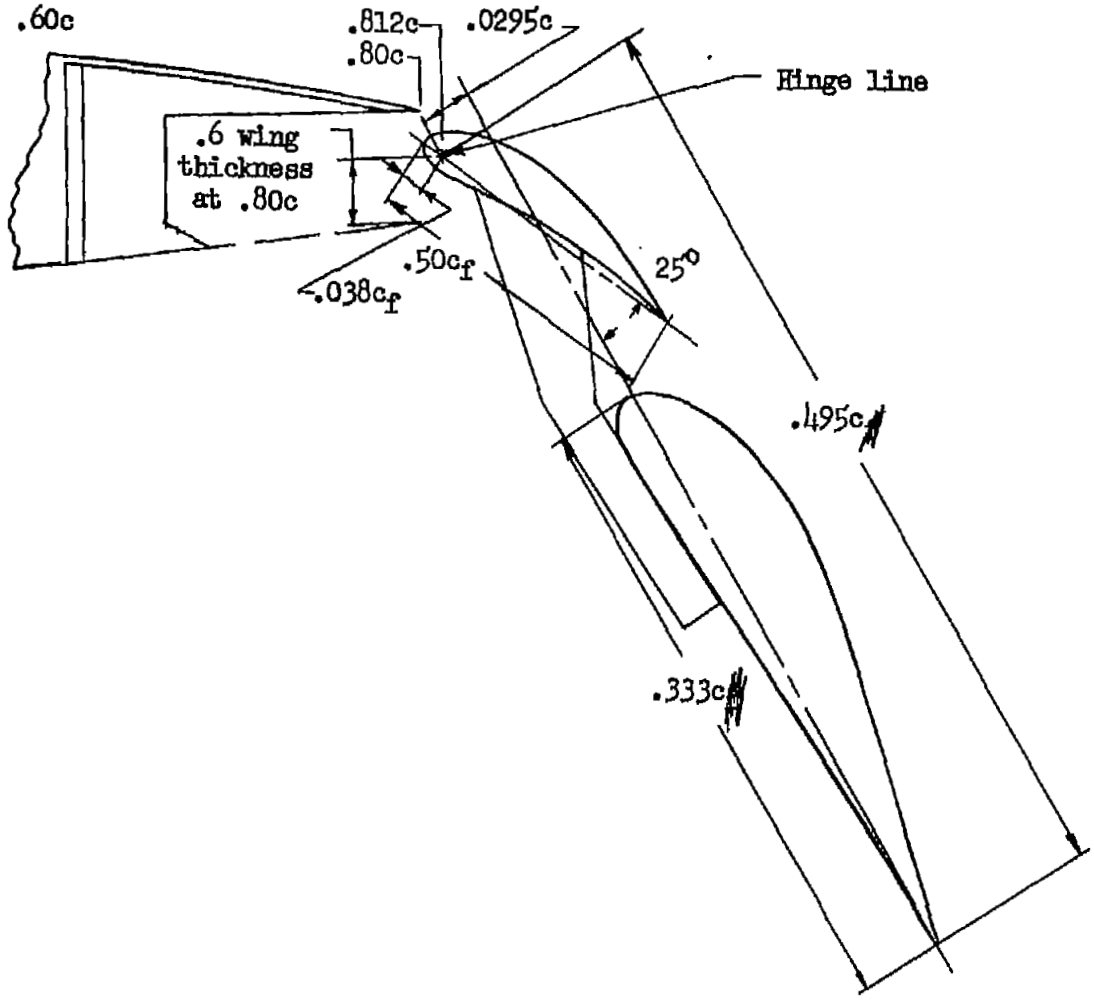

Figure 4.- Details of the double-slotted trailing-edge flap arrangement.

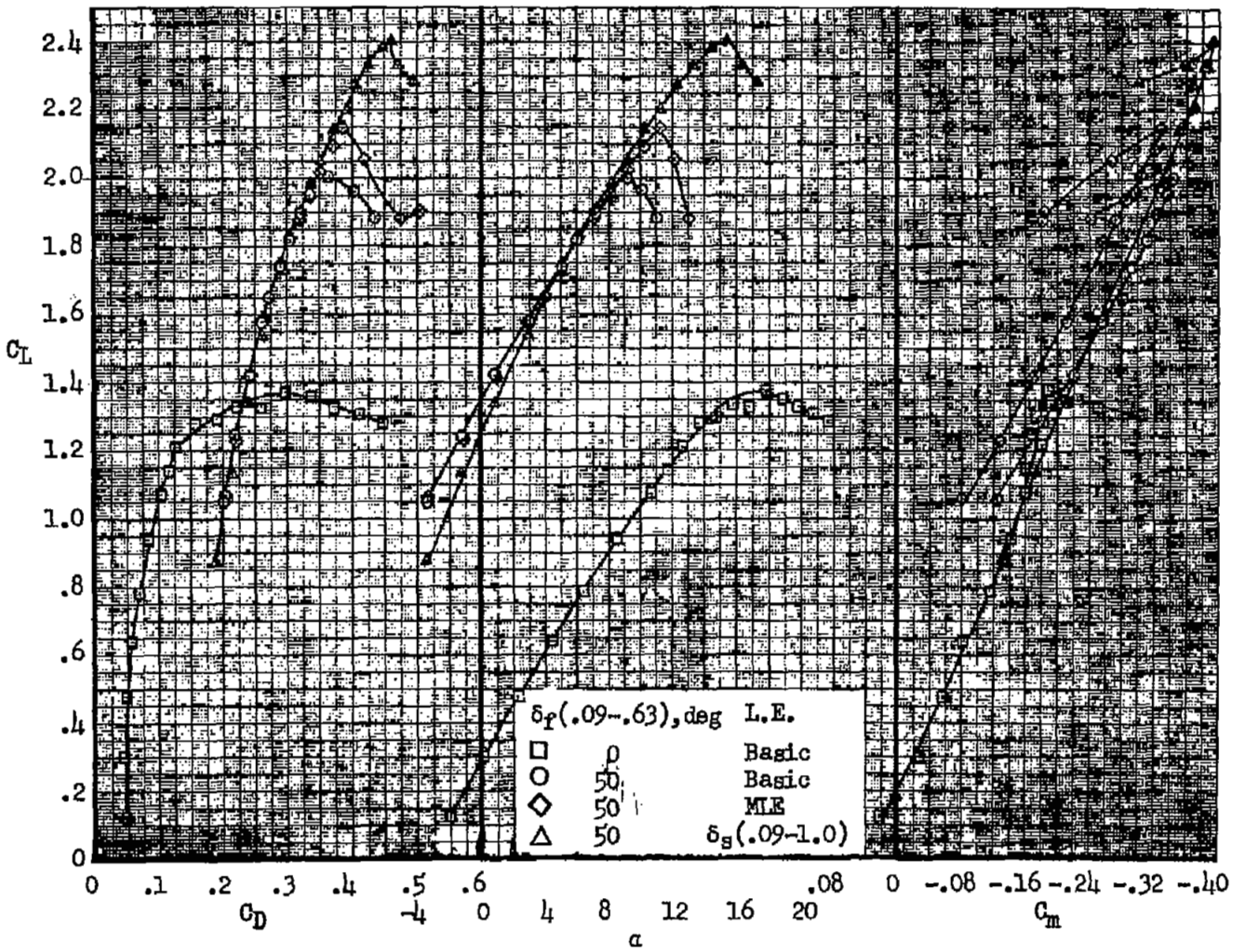

Figure 5.- Longitudinal characteristics of the model with three full-span leading-edge configurations; R = 4.8×10^6.

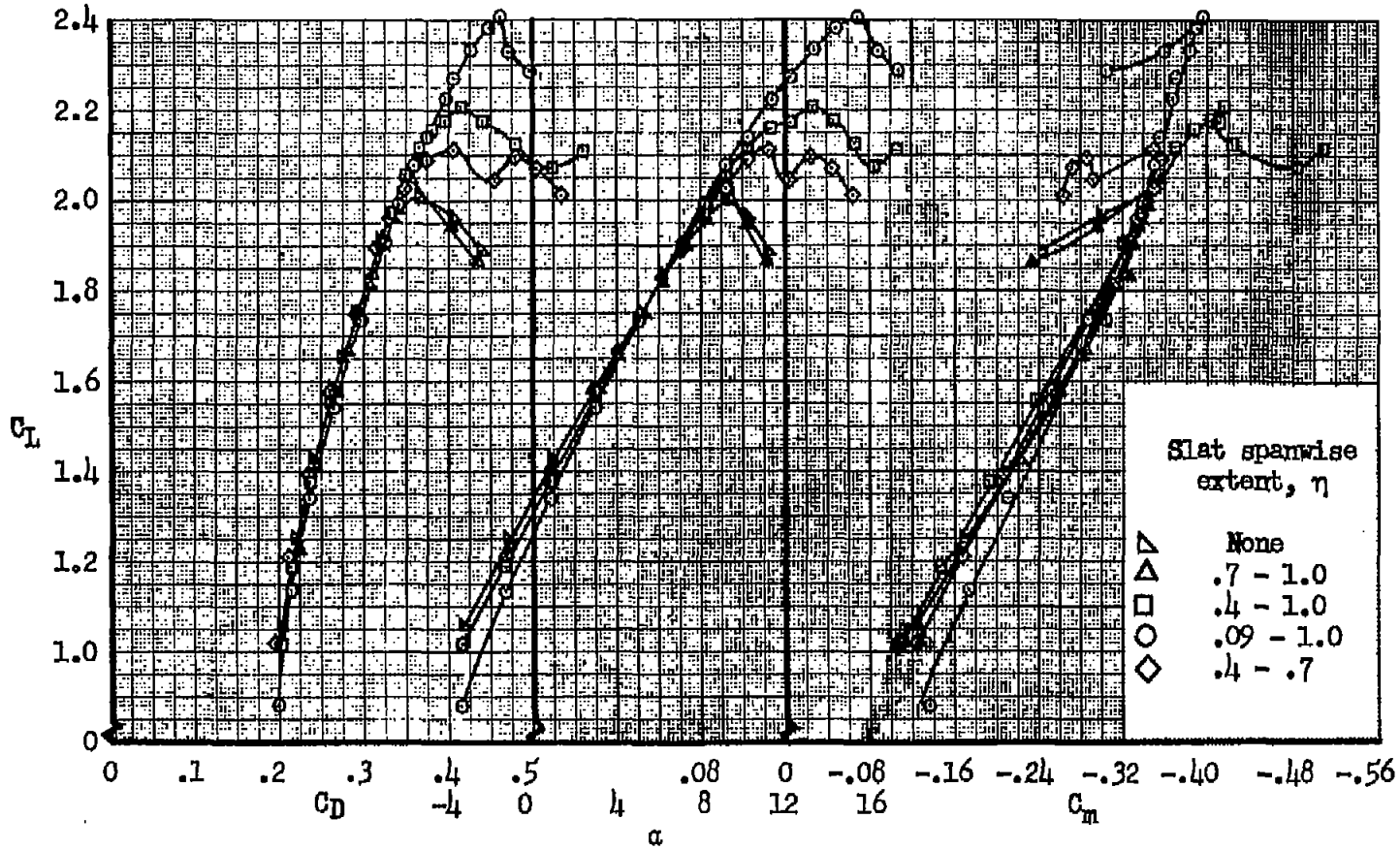

Figure 6.- Effect of spanwise extent of the slats on the longitudinal characteristics of the model; $\delta_f = 50^\circ$ (0.09 - 0.63), $R = 4.8 \times 10^6$.

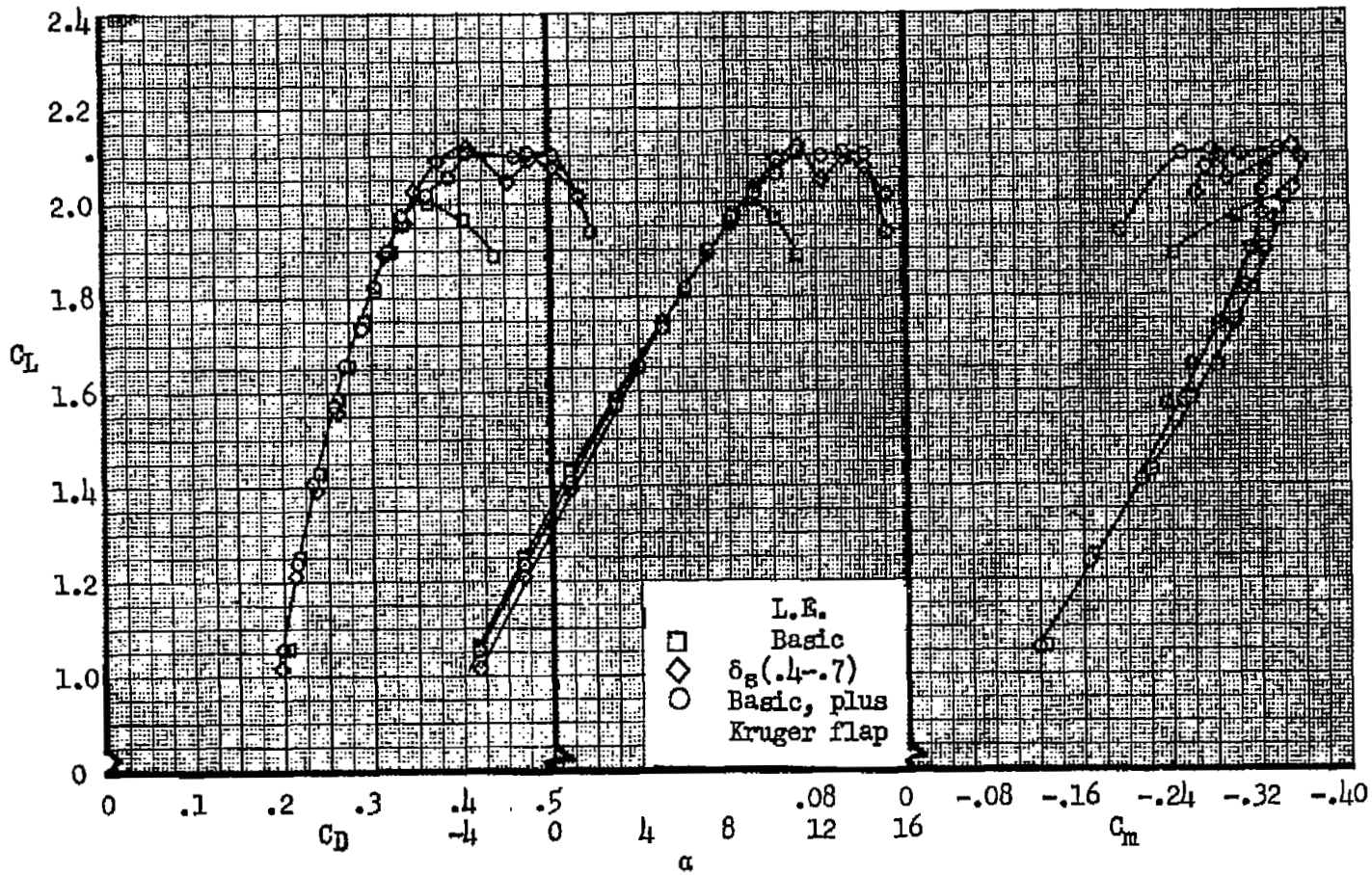

Figure 7.- Effect on longitudinal characteristics of a Kruger flap deflected 50° and extending from η = 0.55 to 0.7; δ_f = 50° (0.09 - 0.63), R = 4.8x10^6.

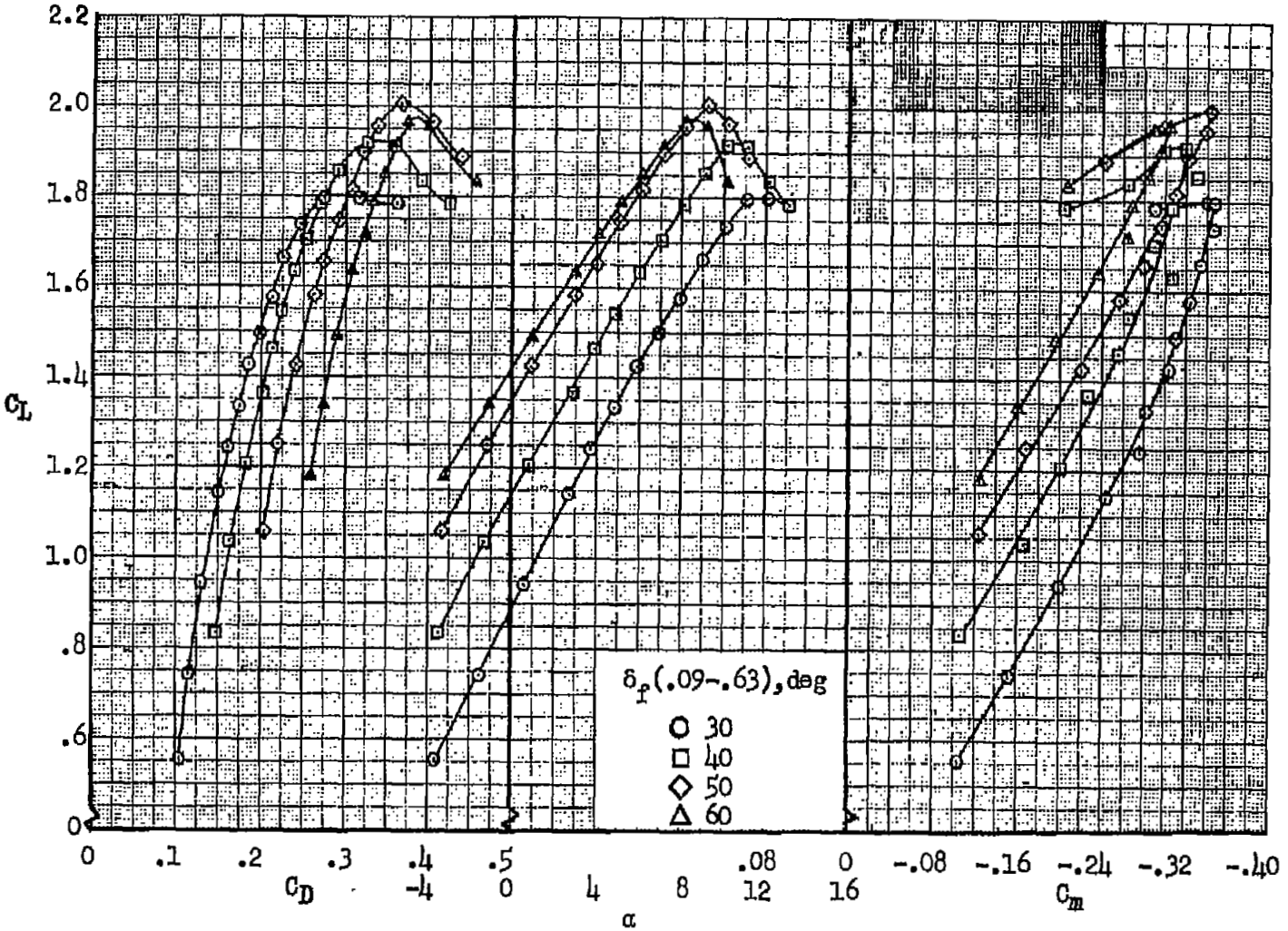

(a) Basic leading edge.

Figure 8.- Effect of trailing-edge flap deflection on longitudinal characteristics; R = 4.8×10^6.

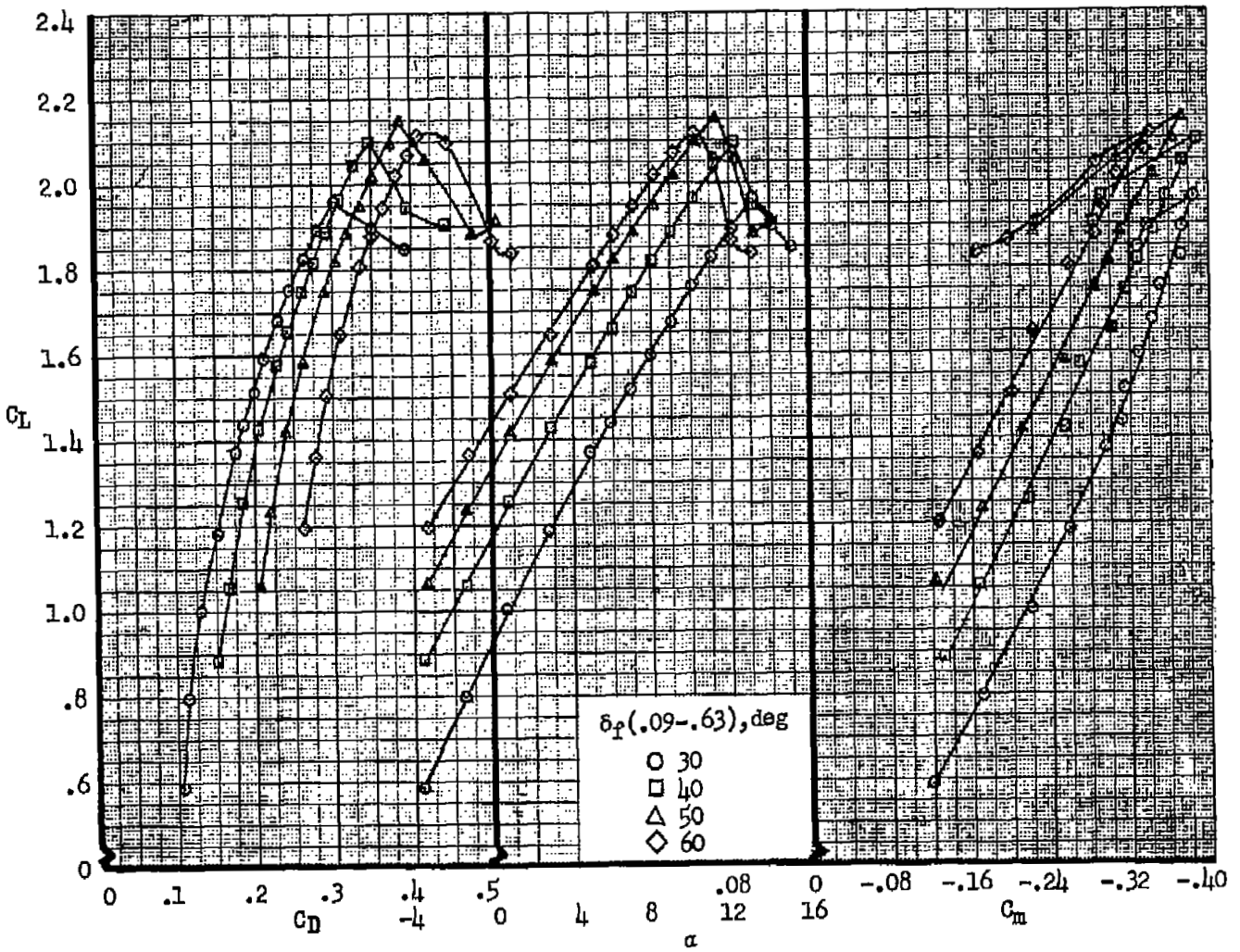

(b) Modified leading edge.

Figure 8.- Continued.

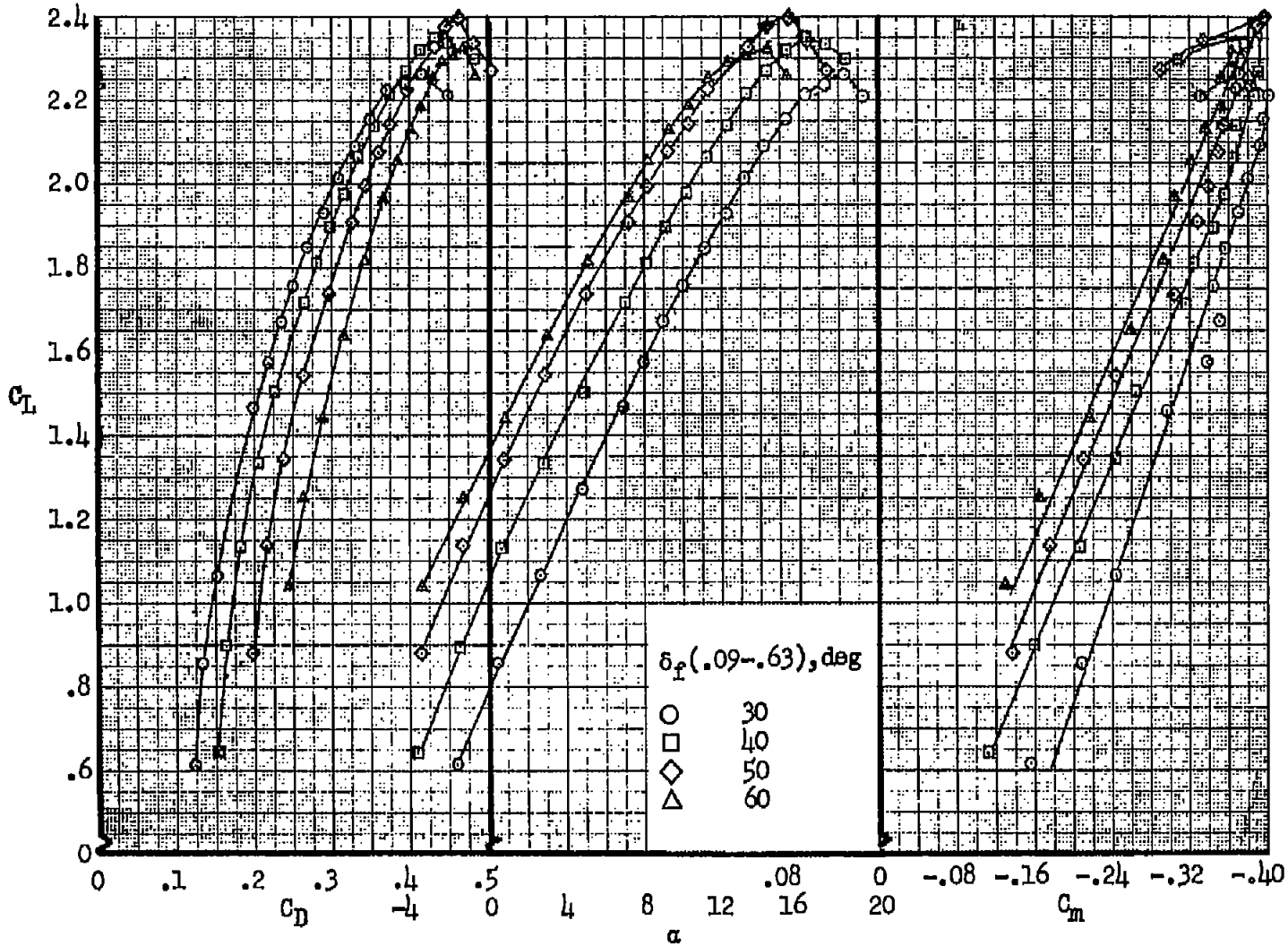

(c) Slats extended.

Figure 8.- Concluded.

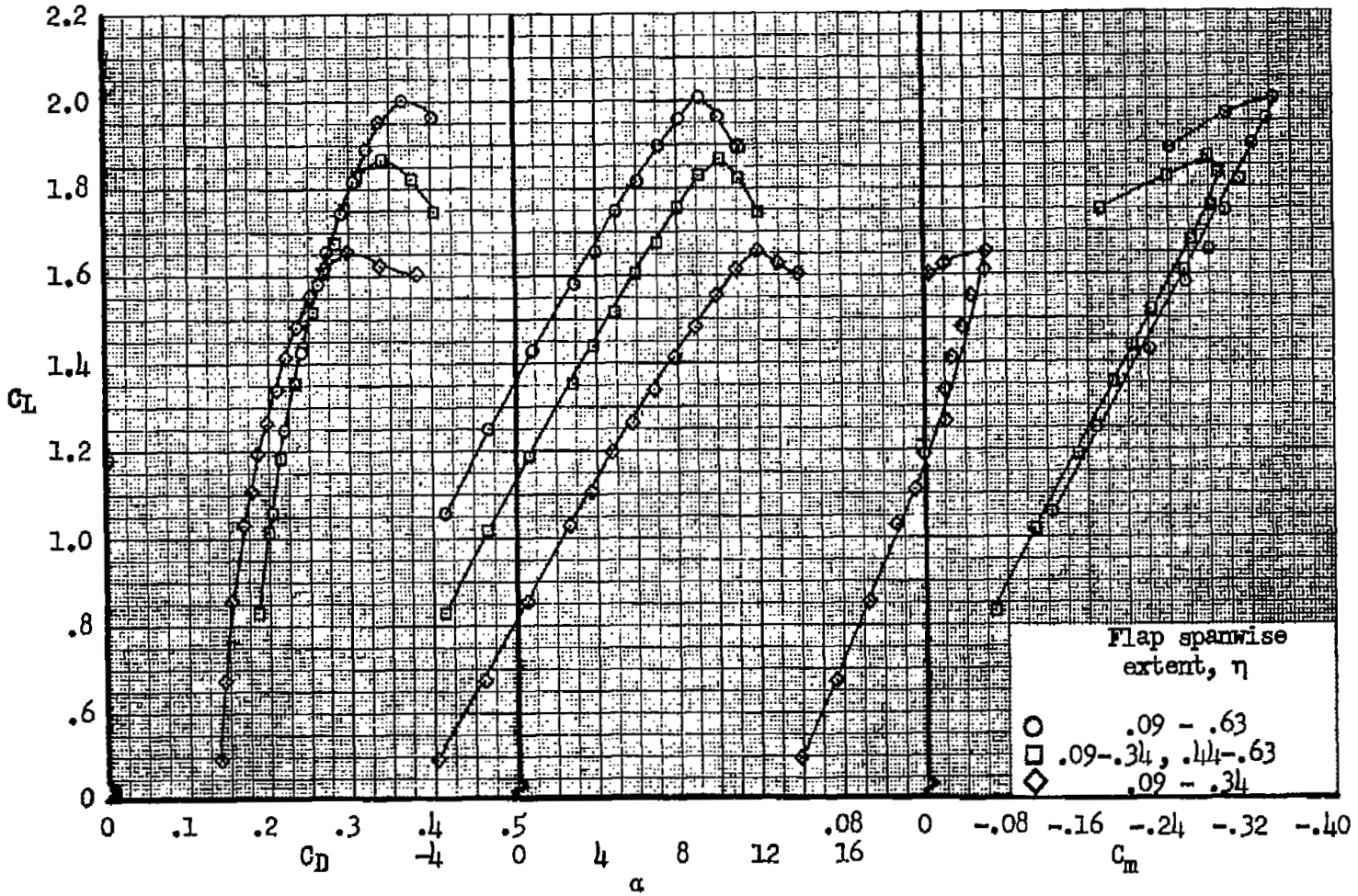

Figure 9.- Longitudinal characteristics with three spanwise extents of trailing-edge flap; plain leading edge, $\delta_f = 50^\circ$, $R = 4.8 \times 10^6$.

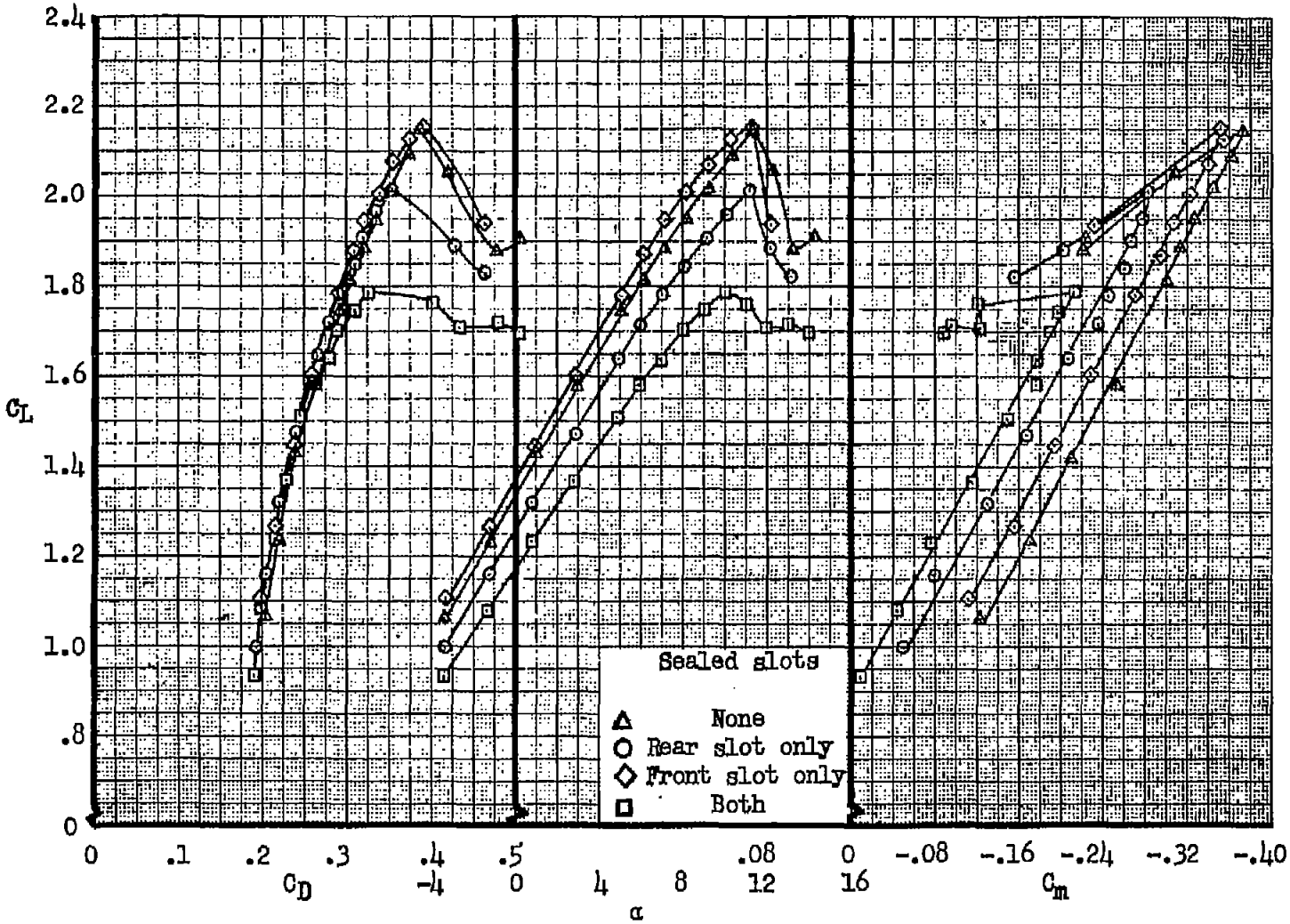

Figure 10.- Effect of blocking trailing-edge flap slots on longitudinal characteristics; modified leading edge, $\delta_f = 50^\circ$ (0.09 - 0.63), R = 4.8×10^6.

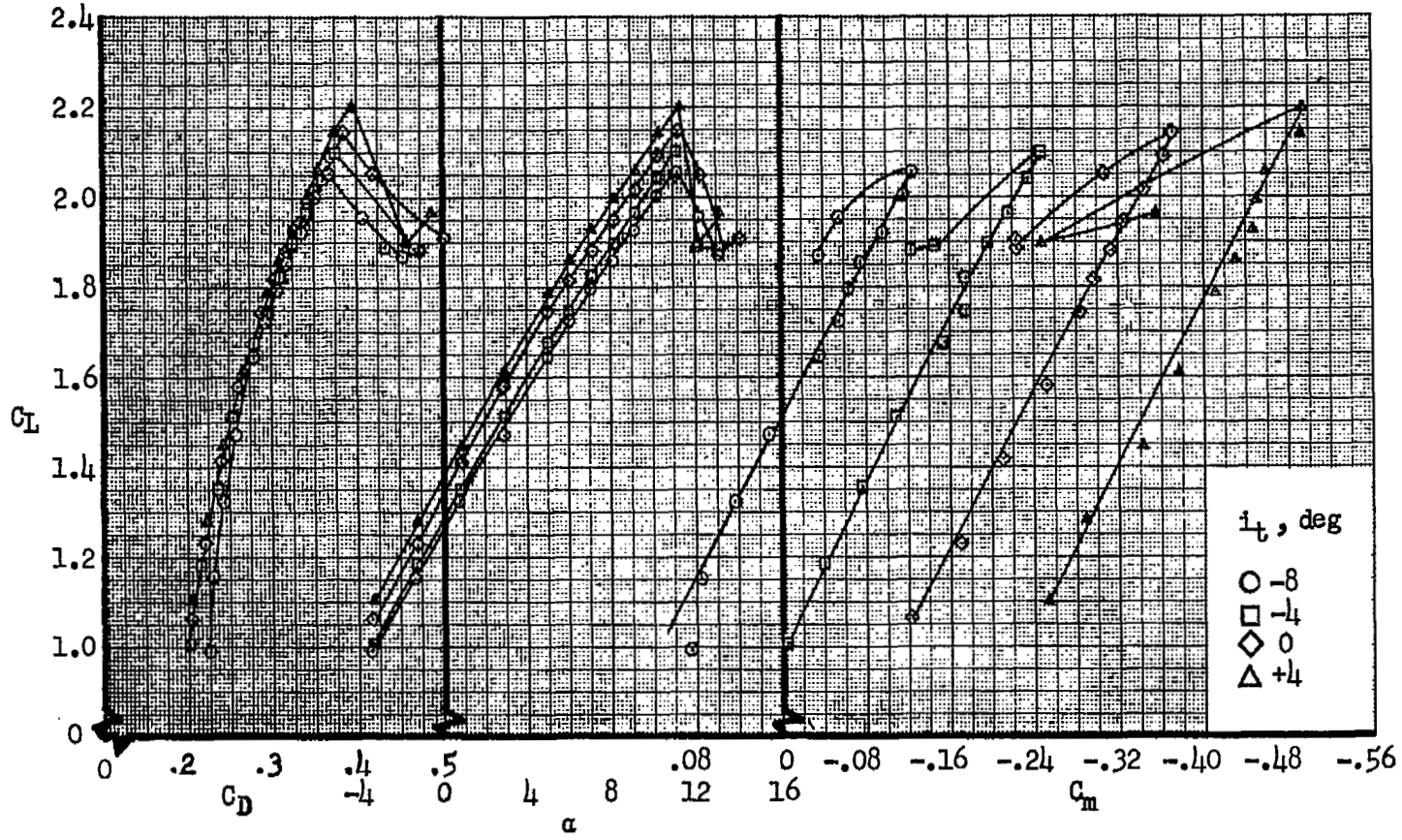

(a) Tail incidence, with modified leading edge.

Figure 11.- Effect of horizontal-tail variables on longitudinal characteristics; $\delta_f = 50^\circ$ (0.09 - 0.63), $R = 4.8 \times 10^6$.

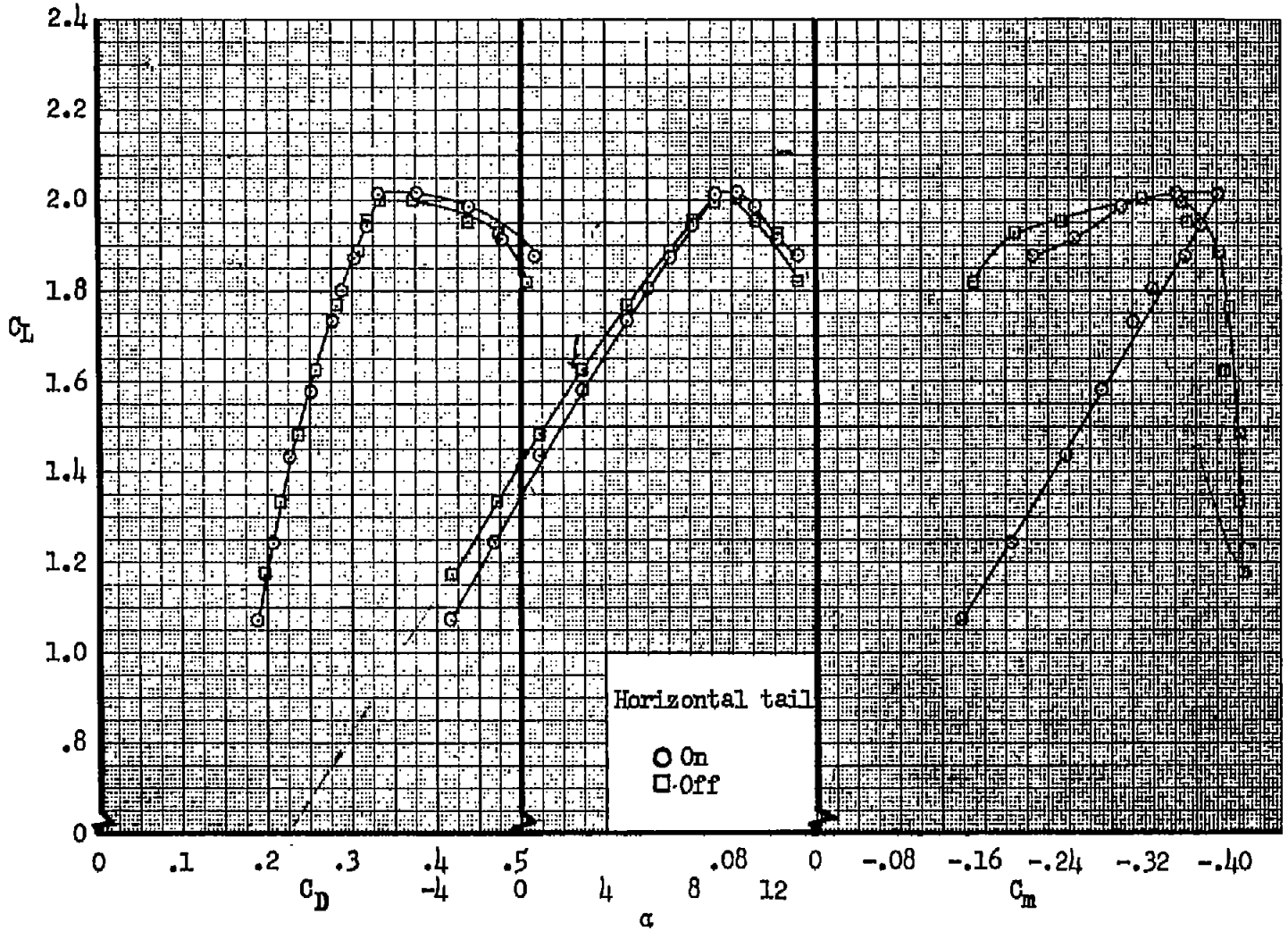

(b) Nacelles off, basic leading edge.

Figure 11.- Concluded.

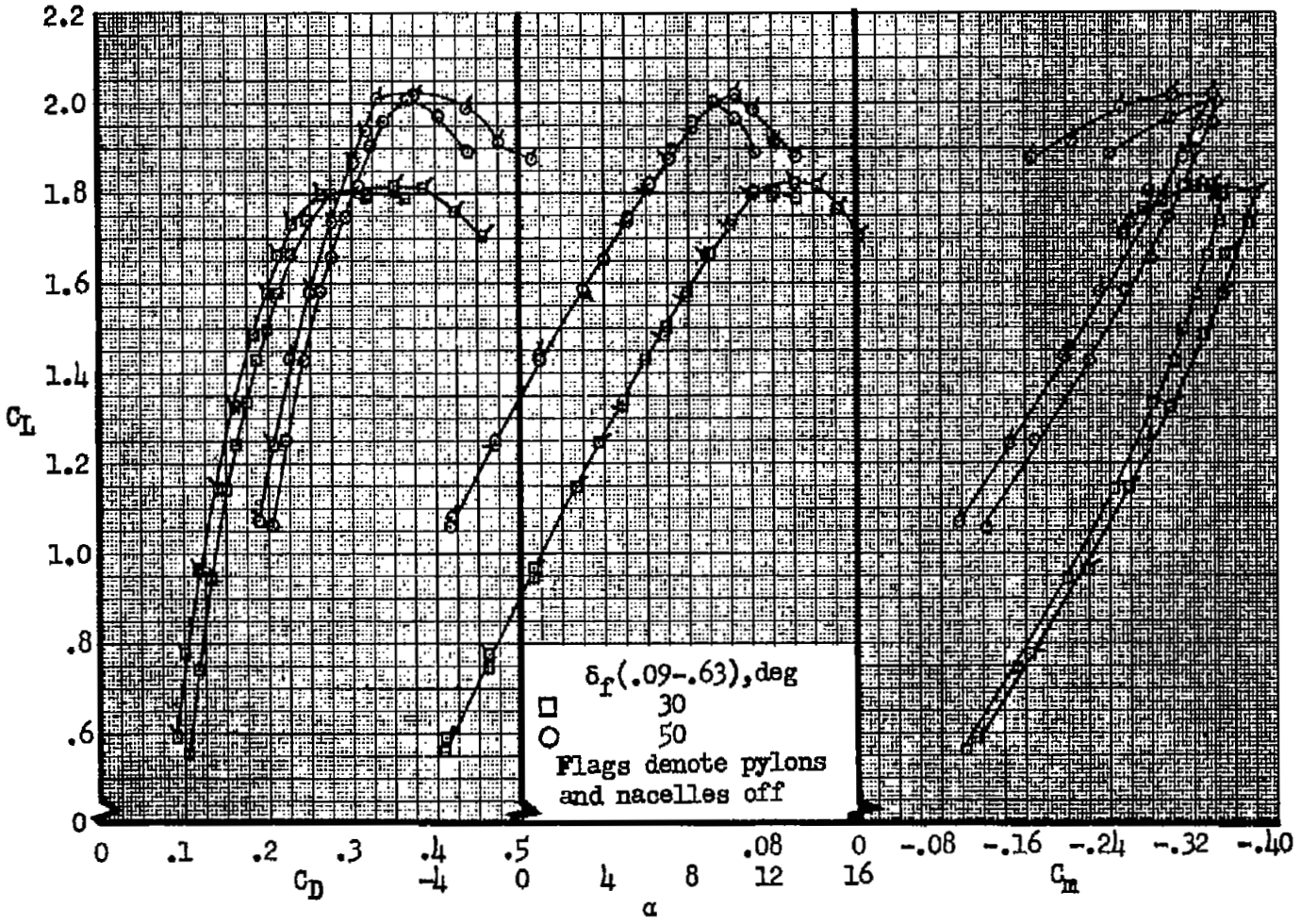

(a) Basic leading edge.

Figure 12.- Effect of pylons and nacelles on longitudinal characteristics.

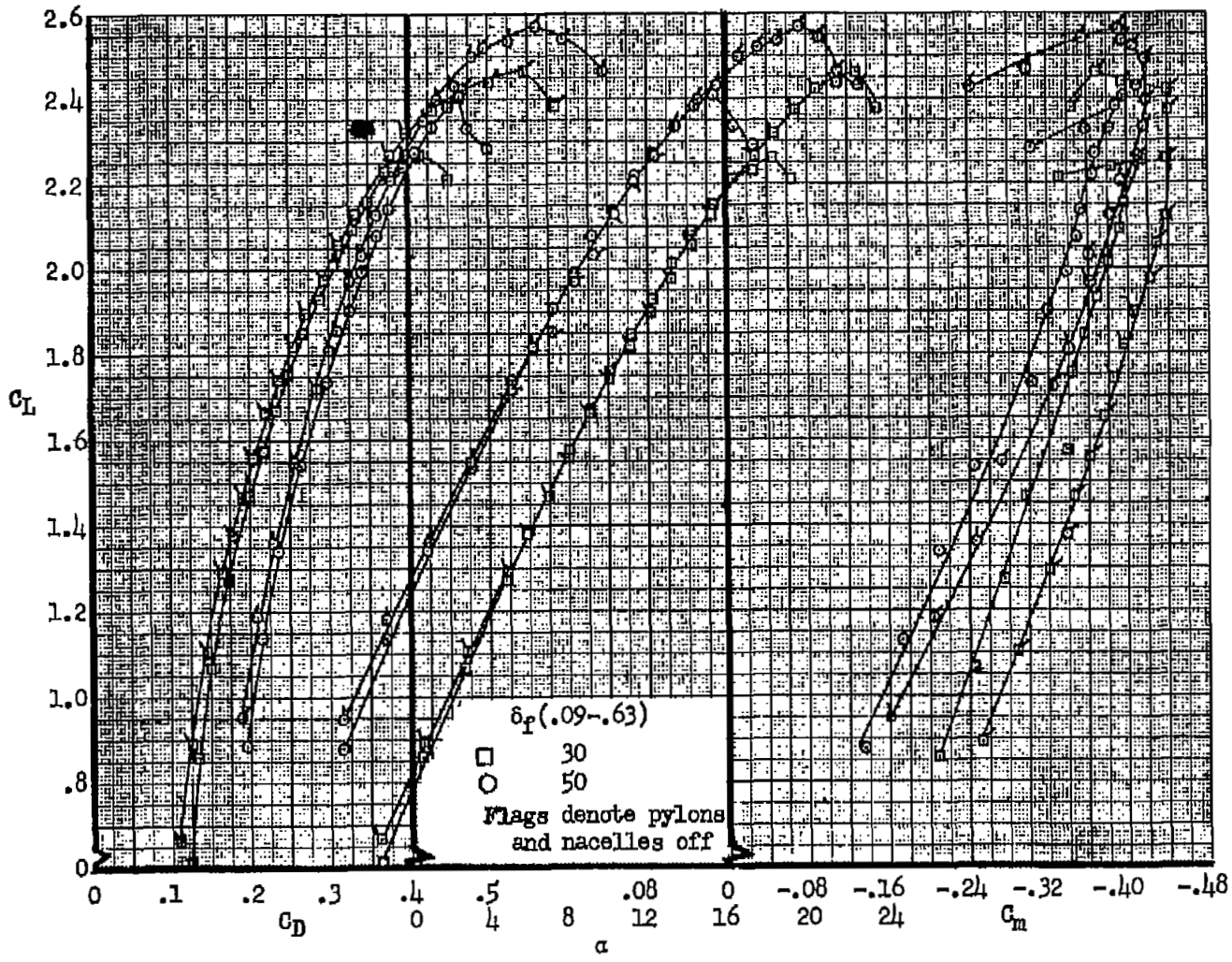

(b) Slats extended.

Figure 12.- Continued.

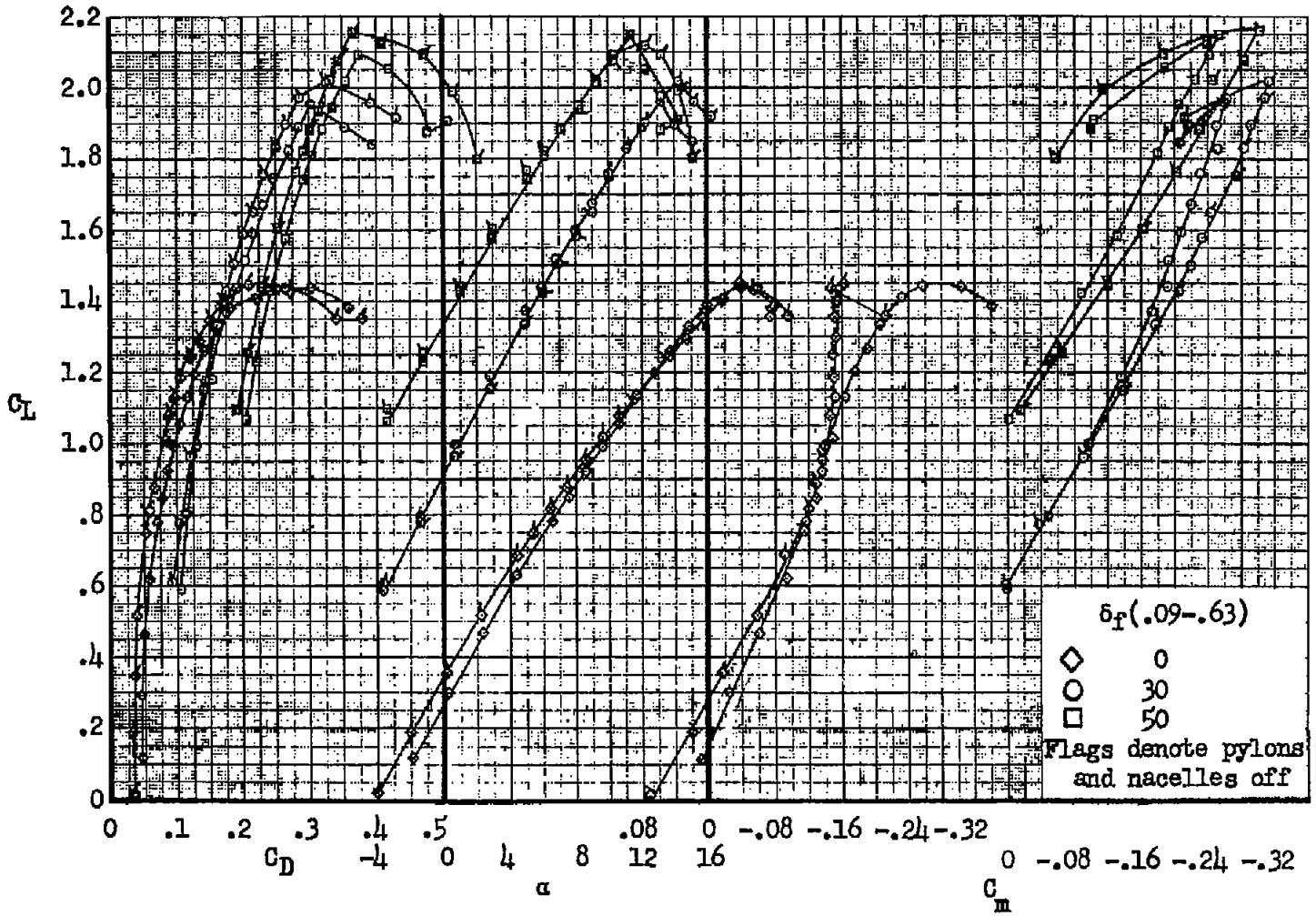

(c) Modified leading edge.

Figure 12.- Concluded.

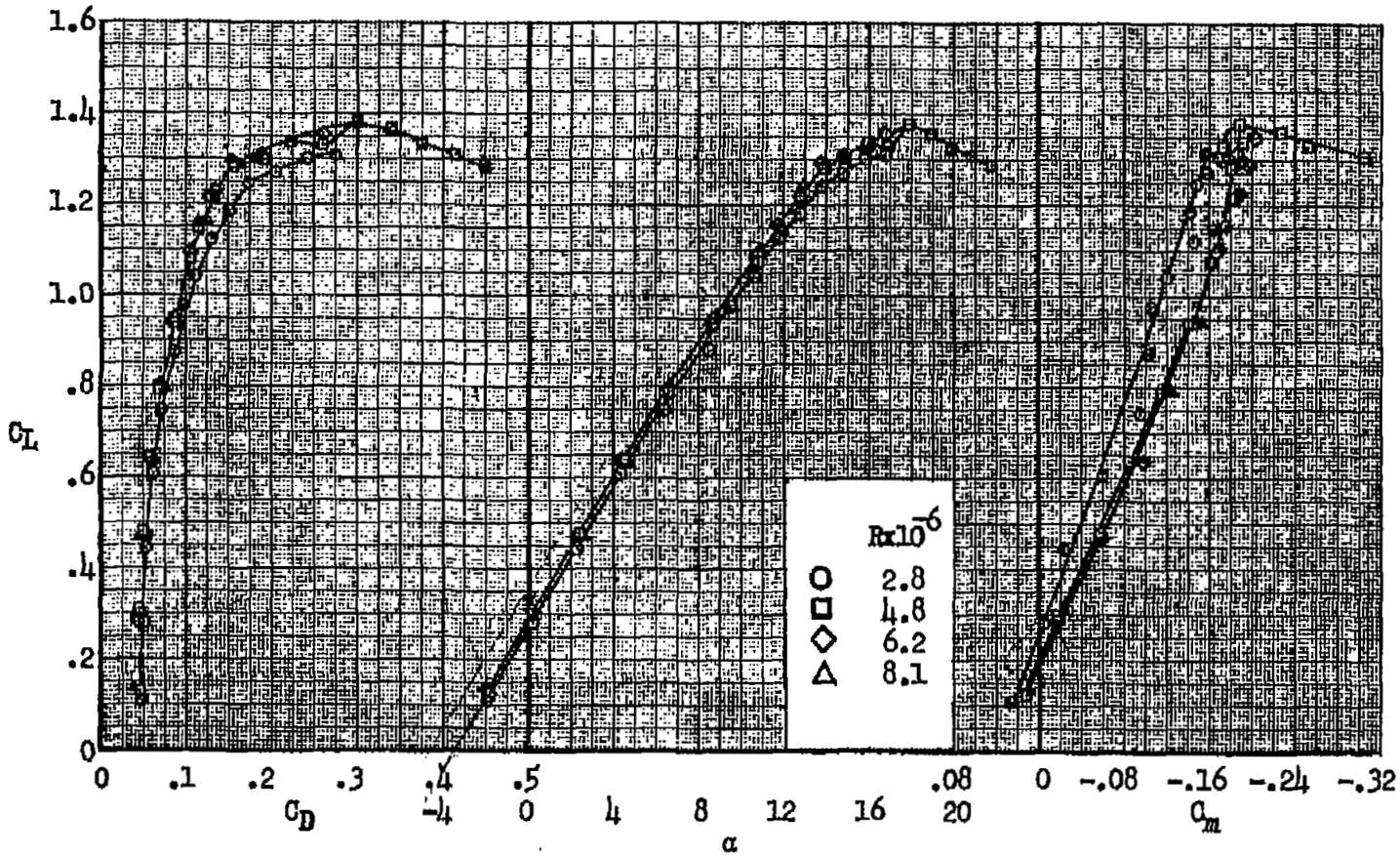

(a) $\delta_f = 0^\circ$

Figure 13.- Effect of Reynolds number on longitudinal characteristics with the plain leading edge.

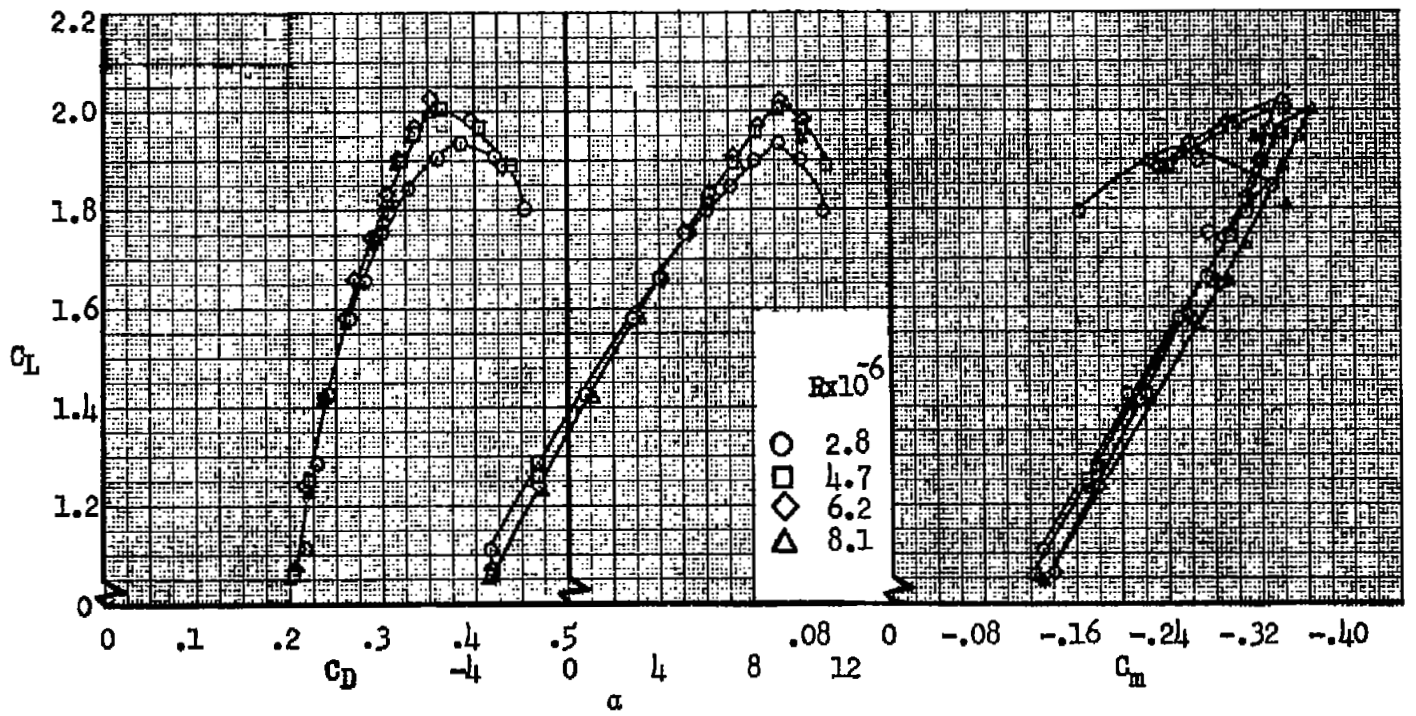

(b) $\delta_f = 50^o$ (0.09 - 0.63)

Figure 13.- Concluded.

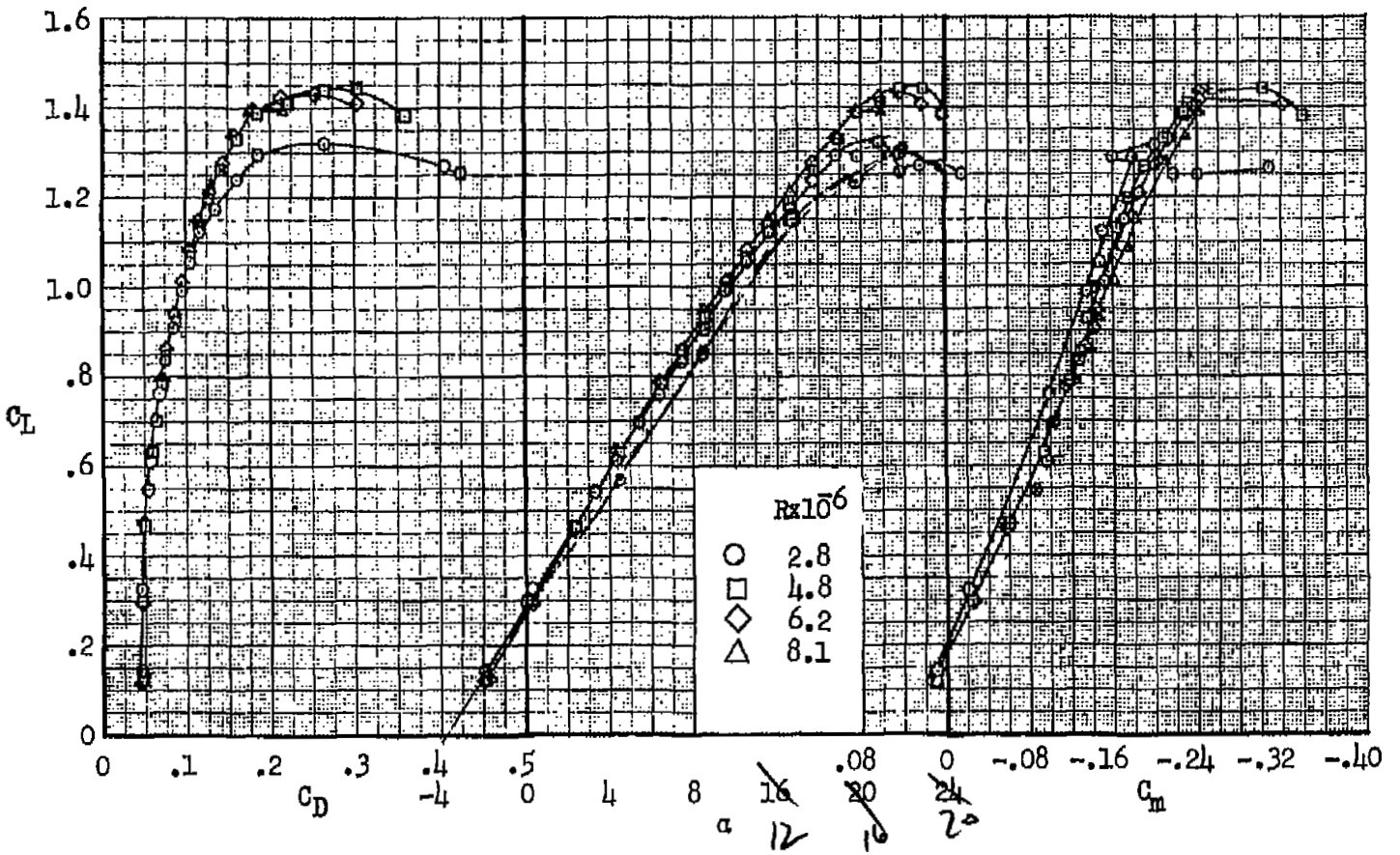

(a) $\delta_F = 0^\circ$

Figure 14.- Effect of Reynolds number with the modified leading edge on longitudinal characteristics.

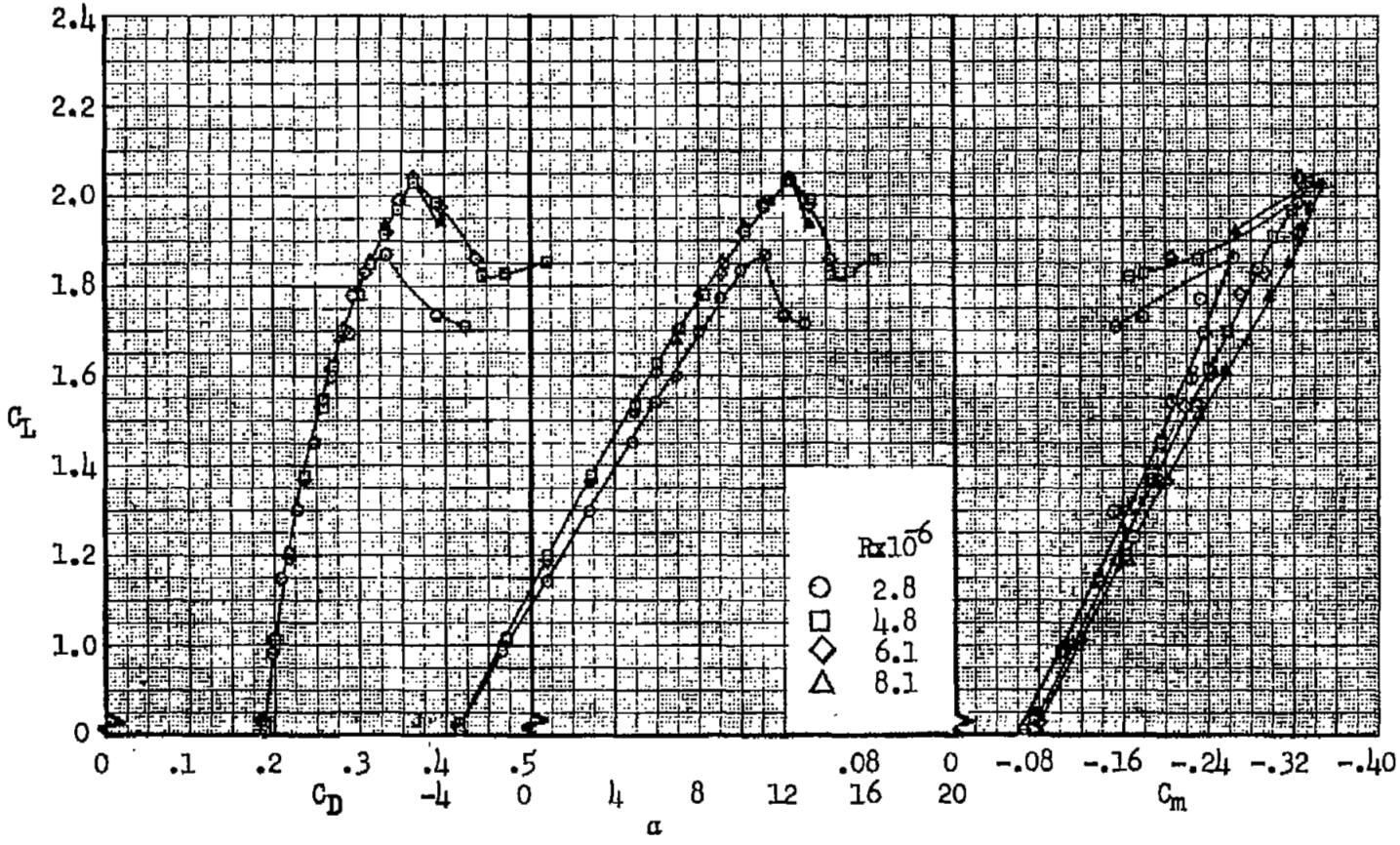

(b) $\delta_f = 50^\circ$ (0.09 - 0.34; 0.44 - 0.63)

Figure 14.- Concluded.

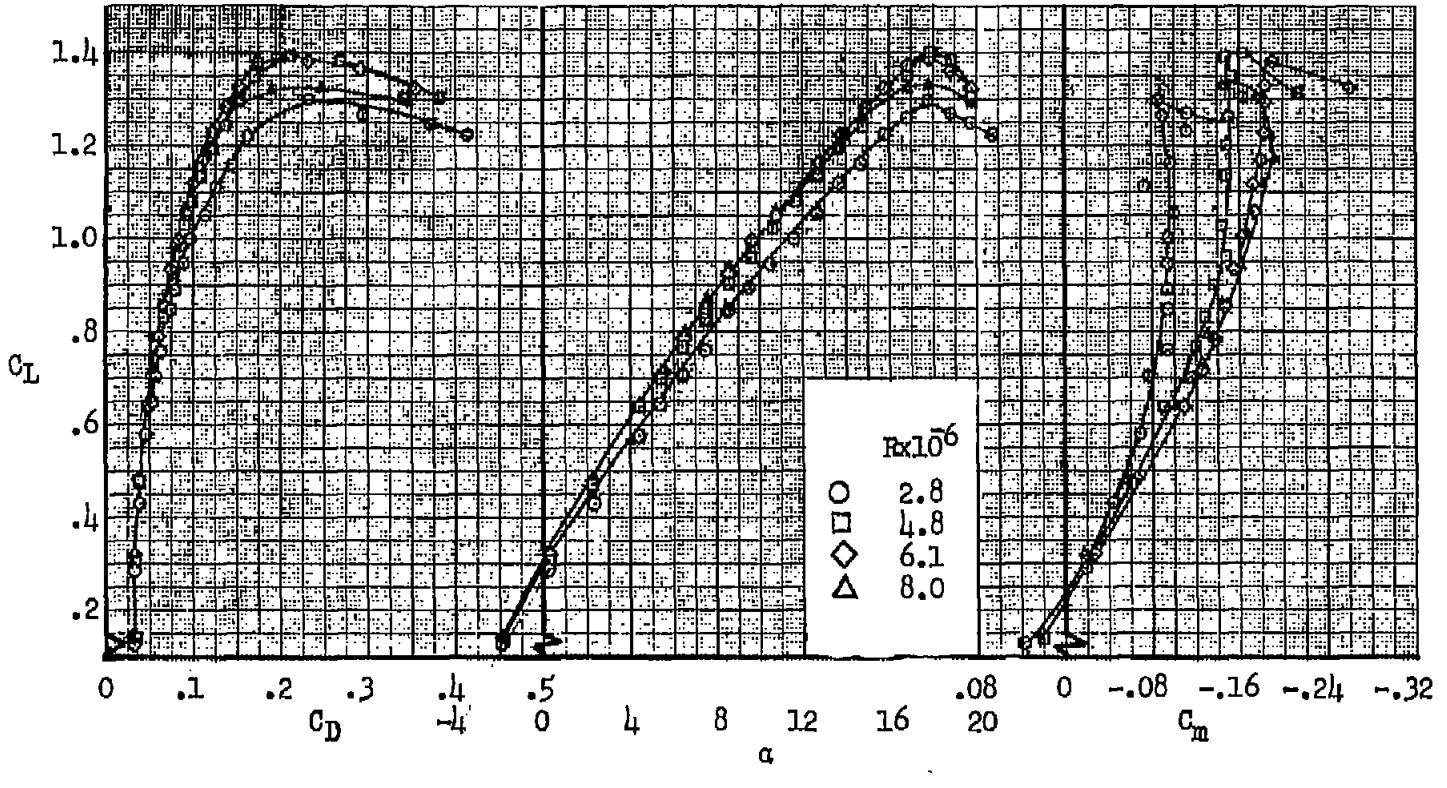

(a) $\delta_f = 0^\circ$

Figure 15.- Effect of Reynolds number on longitudinal characteristics with the modified leading edge and pylons and nacelles removed.

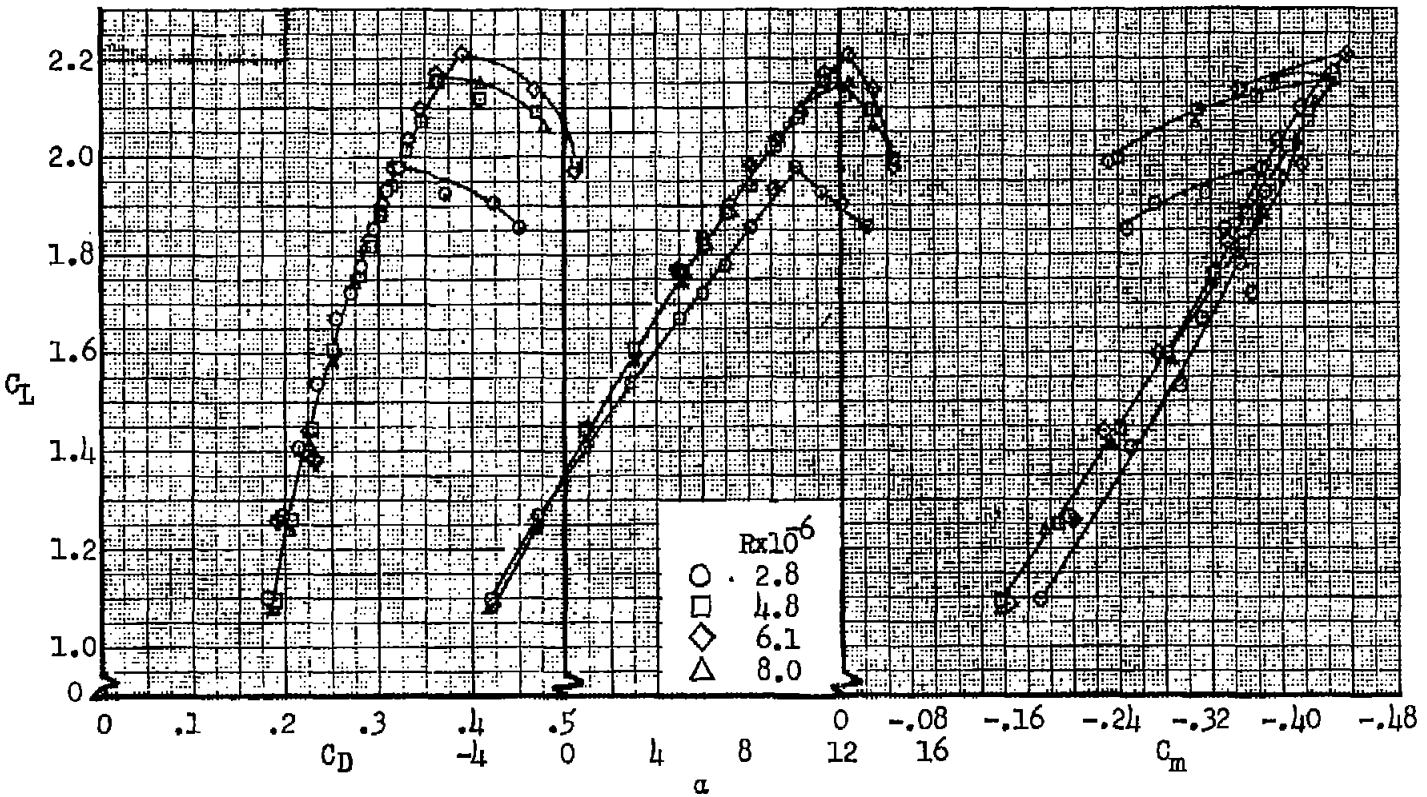

(b) $\delta_f = 50^\circ$ (0.09 - 0.63)

Figure 15.- Concluded.